by Plants. Univ. of Kentucky, Lexington, dissertation, 1975.
8. F.R. Riggle. Soil Water Potential Determination with Thermocouple Psychrometers. Univ. of Minnesota, St. Paul, Master of Agriculture Integrating Paper, March 1978.
9. R.G. McKeen. Evaluation of Swell Characteristics of Airport Pavement Subgrades. Federal Aviation Administration, Final Rept. (in preparation).
10. H.C. Hansen. The Water-Retaining Power of the Soil. Journal of Ecology, Vol. 14, 1926, pp. 111-119.
11. O. Stocker. Uber die Messung von Bodensaughkraften und Ihren Verhaltnis zu den Wurzelsaugkraften. Zeitschrift fuer Botanik, Vol. 23, 1930, pp. 27-56.
12. H. Gradmann. Uber die Messung von Bodensaugwerten. Jahrbuecher fuer Wissenschaftliche Botanik, Vol. 80, 1934, pp. 92-111.
13. R. Gardner. A Method of Measuring the Capillary Tension of Soil Moisture over a Wide Moisture Range. Soil Science, Vol. 43, 1937, pp. 277-283.
14. I.S. McQueen and R.F. Miller. Approximating Soil Moisture Characteristics from Limited Data: Empirical Evidence and Tentative Model. Water Resources Research, Vol. 10, No. 3, June 1974, pp. 521-527.
15. I.S. McQueen and R.F. Miller. Calibration and Evaluation of a Wide-Range Gravimetric Method for Measuring Moisture Stress. Soil Science, Vol. 106, No. 3, 1968, pp. 225-231.
16. R.G. McKeen. Field Studies of Airport Pavement on Expansive Clay. Proc., 4th International Conference on Expansive Soils, Denver, CO, ASCE, New York, Vol. 1, June 1980, pp. 242-261.
17. L.D. Johnson and D.R. Snethen. Evaluation of Soil Suction from Filter Paper. U.S. Army Engineer Waterways Experiment Station, Vicksburg, MS, Miscellaneous Paper GL-80-4, June 1980.
18. R.L. Lytton. The Characterization of Expansive Soils in Engineering. Presented at Symposium on Water Movement and Equilibrium in Swelling Soils, American Geophysical Union, San Francisco, Dec. 1977.
19. R.G. McKeen and J.P. Nielsen. Characterization of Expansive Soils for Airport Pavement Design. Federal Aviation Administration, Rept. FAA-RD-78-59, Aug. 1978.
20. G.D. Aitchison, P. Peter, and R. Martin. Quantitative Description of the Stress Deformation Behavior of Expansive Soils. Proc., 3rd International Conference on Expansive Soils, Haifa, Israel, 1973.
21. D.G. Fredlund. Appropriate Concepts and Technology for Unsaturated Soils. Canadian Geotechnical Journal, Vol. 16, No. 1, Feb. 1979, pp. 121-138.
22. D.G. Fredlund, J.U. Hasan, and H.L. Filson. The Prediction of Total Heave. Proc., 4th International Conference on Expansive Soils, Denver, CO, ASCE, New York, Vol. 1, June 1980, pp. 1-17.
23. P.V. Compton. A Study of the Swelling Behavior of an Expansive Clay as Influenced by the Clay Microstructure, Soil Suction, and External Loading. Texas A&M Univ., College Station, dissertation, 1970.
24. V. Escario and J. Saez. Measurement of the Properties of Swelling and Collapsing Soils Under Controlled Suction. Proc., 3rd International Conference on Expansive Soils, Haifa, Israel, 1973, pp. 195-200.
25. Soil Survey Laboratory Data and Descriptions for Some Soils of Arizona. Soil Conservation Service, U.S. Department of Agriculture, Soil Survey Investigations Rept. 28, Aug. 1974.
26. Soil Survey Laboratory Data and Descriptions for Some Soils of California. Soil Conservation Service, U.S. Department of Agriculture, Soil Survey Investigations Rept. 24, June 1973.
27. Soil Survey Laboratory Data and Description of Some Soils of Texas. Soil Conservation Service, U.S. Department of Agriculture, Soil Survey Investigations Rept. 30, Jan. 1976.
28. J.R. Pearring. A Study of Basic Mineralogical, Physical-Chemical, and Engineering Index Properties of Laterite Soils. Texas A&M Univ., College Station, dissertation, Aug. 1963.
29. J.H. Holt. A Study of Physico-Chemical, Mineralogical, and Engineering Index Properties of Fine-Grained Soils in Relation to Their Expansive Characteristics. Texas A&M Univ., College Station, dissertation, May 1969.
30. A.A. Porter. The Mechanics of Swelling in Expansive Clays. Colorado State Univ., Fort Collins, thesis, May 1977.
31. D.E. McCormack and L.P. Wilding. Soil Properties Influencing Swelling on Canfield and Geeburg Soils. Proc., Soil Science Society of America, Vol. 39, No. 3, May-June 1975, pp. 496-502.
32. C. McDowell. Interrelationship of Load, Volume Change, and Layer Thicknesses of Soils to the Behavior of Engineering Structures. Proc., HRB, Vol. 35, 1956, pp. 754-772.
33. D.J. Weston. Expansive Roadbed Treatment for Southern Africa. Proc., 4th International Conference on Expansive Soils, Denver, CO, ASCE, New York, Vol. 1, June 1980, pp. 339-360.
34. Guide to the Use of the Soil PVC Meter. Federal Housing Administration, Tech. Studies Rept. 595, Jan. 1965.

Publication of this paper sponsored by Committee on Environmental Factors Except Frost.

Pavement Roughness on Expansive Clays

M.O. VELASCO AND R.L. LYTTON

The roughness patterns of pavements on expansive-clay subgrades were measured by using the General Motors profilometer on 20 sections of pavement in Texas. The roughness patterns are analyzed by means of two methods: the Fast Fourier Transform and a technique that reproduces a rod-and-level survey. The analysis shows that the roughness of expansive clays can be viewed as a spectrum of sine wave amplitudes that vary directly with their corresponding

wave lengths. The spectra for each pavement section are fitted by an equation that has two constants: a coefficient and a power. The values of these two constants are found by regression analysis to depend on the flexural stiffness of the pavement, time, climate, and several physicochemical soil properties. An equation that can predict loss of pavement serviceability index was also determined by regression analysis to depend on the same pavement, climate, and soil properties. An example of the use of this equation in the prediction of the performance of a pavement on expansive clay is given, and its implications for pavement design are discussed.

The practical consequences of pavement roughness caused by expansive clay are loss of riding comfort and reduction in pavement service life.

The genesis of the waves observed on these pavements can be understood by studying a common landform that develops in some climatic areas that have expansive clays. This undulating surface, characterized by a pattern of mounds and depressions, has been called "gilgai". Beckmann and others (1) have studied several types of this landform and factors that influence their genesis. In addition, Lytton and others (2) have described the stages of development of normal gilgai in their study of two gilgai fields in Texas. These authors conclude that the cracking fabric of the soil is the principal factor in the appearance and behavior of the gilgaied landform and that the crack spacing of the soil depends on its mineralogy. When a roadway is constructed on a soil that has the potential to develop gilgai, its cracking pattern will usually remain beneath the roadway. If water has access to the soil mass, differential movements may take place and then pavement roughness will appear. For example, in the study of the two Texas gilgai fields cited above, pavement roughness was also measured on pavement sections adjacent to the fields. Statistical analyses of these data showed that the probability density functions of the pavement wavelengths were similar to those determined in the gilgai fields, which indicated that the same roughness patterns were developing beneath the pavement (2).

It is clear that the first steps in dealing with the complexity of pavement design on expansive soils are to collect consistent measures of pavement roughness and characterize them in a useful manner. The results of the analysis of pavement roughness on 20 roadway sections located in nine different areas of central Texas are reported in this paper.

Central Texas belongs to the Atlantic and Gulf Coastal Plain physiographic province, which is underlain by a sequence of sedimentary rocks and nonlithified sediments. In central Texas, this sequence contains some highly expansive argillaceous rocks (3). Soils included in the Vertisol order are also abundant in this area. The climate varies widely, as indicated by the range of mean Thornthwaite Moisture Index values: normally between 20 and -20.

Study of the measured pavement roughness by using Fast Fourier Transforms (FFTs) reveals that the overall patterns of roughness can be characterized as a function of only two parameters: a coefficient c and a power n. The development of empirical models to predict the values of these two parameters as a function of the characteristics of the pavement, time, climate, and several physicochemical soil properties leads to a better understanding of the factors that influence the appearance of roughness. As a basis for a design procedure, the two parameters are correlated with the reduction in the serviceability index. An analysis of the dominant wavelengths present in the roughness patterns shows that there are several such wavelengths that are common to all pavements.

CHARACTERIZATION OF ROUGHNESS

The General Motors profilometer was used to measure the profiles of the 20 pavement sections. Road profiles for both right and left wheel paths were converted to digital form and stored on magnetic tapes. In this study, a segment of the available profile in each section has been analyzed by using the FFT. Basically, the FFT decomposes the road profile into a family of sinusoidal functions at discrete frequencies. A complete description of this mathematical tool can be found in the literature (4,5). For this study, an FFT computer program was designed to perform the following operations in each profile:

1. Sample the profile at equally spaced intervals of 0.82 ft (0.25 m);
2. Take 512 of those data samples, which represent a length of 419.84 ft (128 m);
3. Apply the FFT algorithm to that length, obtaining the distribution of one-half the amplitude values (A/2) of sinusoids at the following frequencies:

$$f = j/419.84 \quad j = 2, 3, 4, \ldots, 511 \tag{1}$$

where f is in cycles per foot;

4. Repeat operations 2 and 3 for 10 consecutive lengths, with the first points of each separated by 164 ft (50 m), so that the 10 lengths cover 1896 ft (578 m) of the road profile (in a few sections, the available profile was less than 1896 ft long, and for these a smaller number of lengths with a minor separation were considered); and
5. Average the distributions of A/2 values calculated for the different lengths and print out the results.

Besides having an easily understandable physical meaning, these mean spectra of A/2 over the frequency domain are a very useful representation of the measured roughness of the pavement sections (see Figure 1). Furthermore, the shapes of the spectra that were obtained strongly suggested that they may be fitted by curves defined by the following general equation:

$$A/2 = c f^{-n} \tag{2}$$

where A is the amplitude (in inches) of a sinusoid with frequency f and c and n are parameters.

If one takes logarithms of both sides of the equation, it becomes the general equation of a straight line with slope equal to -n and intercept equal to log c. Thus, linear regression analysis was used, for the measured A/2 versus f spectrum in each roadway segment, to determine the corresponding n and log c values. All of the R^2 values were above 0.90. The values of the parameters completely characterize the pattern of roughness in each pavement section. In Figures 2 and 3, the straight lines that represent the roughness spectra for the right and left wheel paths of the different pavement sections are shown, with wavelength instead of frequency in the abscissa axis. The relation between wavelength (λ) and frequency (f) is $\lambda = 1/f$. For a specific roadway segment, it can be seen from these two figures that the roughness spectra of the right and left wheel paths are very similar. Nevertheless, for most of the sections the spectrum of the right wheel path indicates a slightly greater roughness (greater amplitudes over the wavelength domain) than in the left wheel path. This point can be roughly illustrated by calculating the average of the straight lines presented in

Figure 2 and comparing it with the average of those in Figure 3. This comparison is shown in Figure 4. The fact that more roughness generally develops in the right wheel path seems reasonable, since the right wheel path is closer to the edge of the pavement, where greater variations in soil moisture are likely to occur.

It appears that c and n are not only complementary parameters of the same phenomenon but are also not truly independent. To analyze this possibility, the log c values have been plotted versus the correspondent n values for the right wheel path of all of the roadway sections. Figure 5 shows a general tendency of the absolute value of n to decrease when the log c value increases. Furthermore, in several roadway sections in the San Antonio area, roughness was measured on different dates. The correspondent log c and n values on different dates for each section are fitted by straight lines with the same slope. The general equation of these straight lines is

$$\log c = \log c_1 + 2.02n \quad (3)$$

where log c_1 is the intercept in the log c versus n plot. If it is assumed that Equation 3 holds true also for the rest of the roadway sections (where roughness measures on different dates are not available), it becomes evident that log c and n are not independent. Moreover, the intercept (log c_1) in Equation 3 is probably related to some of the factors causing roughness that do not vary with time, such as soil properties.

Dominant Wavelengths

Lytton and others (2) and McKeen (6) have suggested that the pavement-roughness spectra on expansive soils tend to show some dominant wavelengths. Although the influence of these wavelengths will be reflected in the values of log c and n, it is also interesting to distinguish them specifically.

A simple assumption is made that the measured

Figure 1. Frequency domain of amplitude values (Buckholts 1 test section).

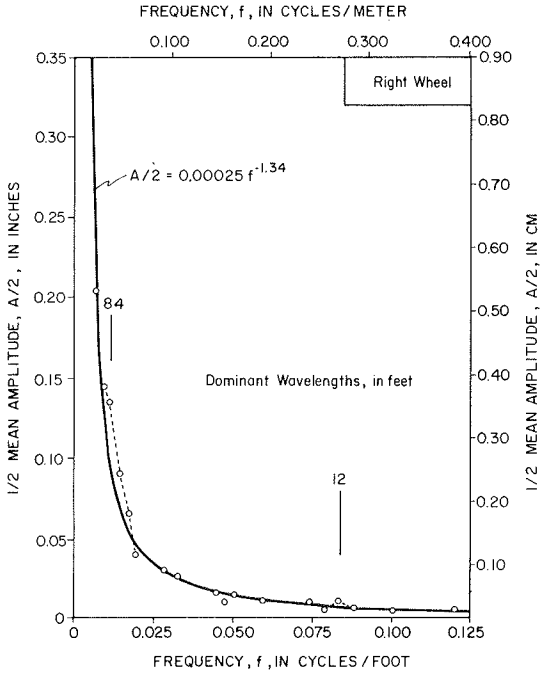

Figure 2. Roughness spectra for right wheel path.

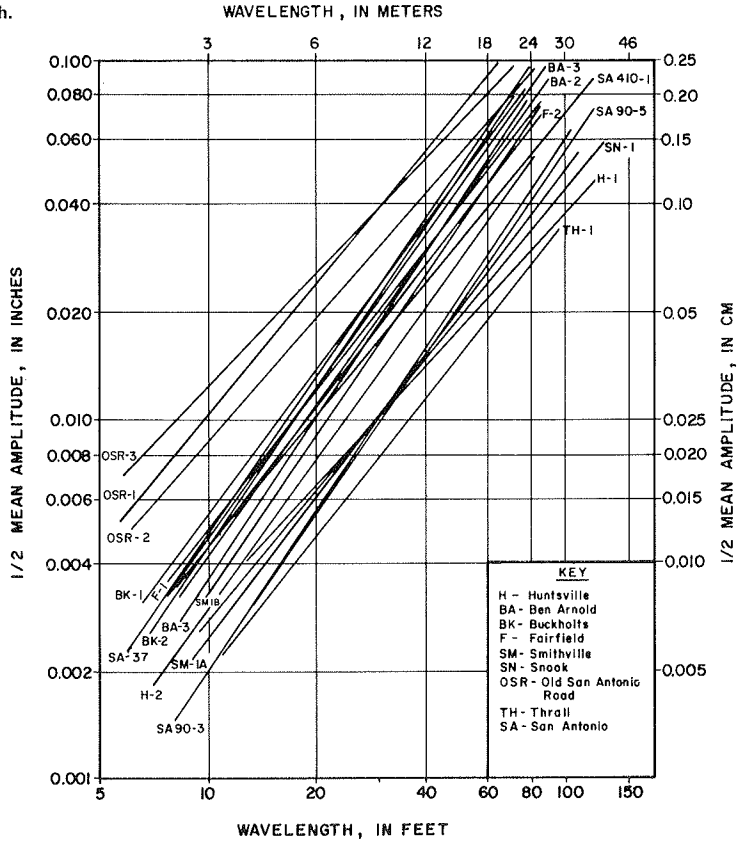

Figure 3. Roughness spectra for left wheel path.

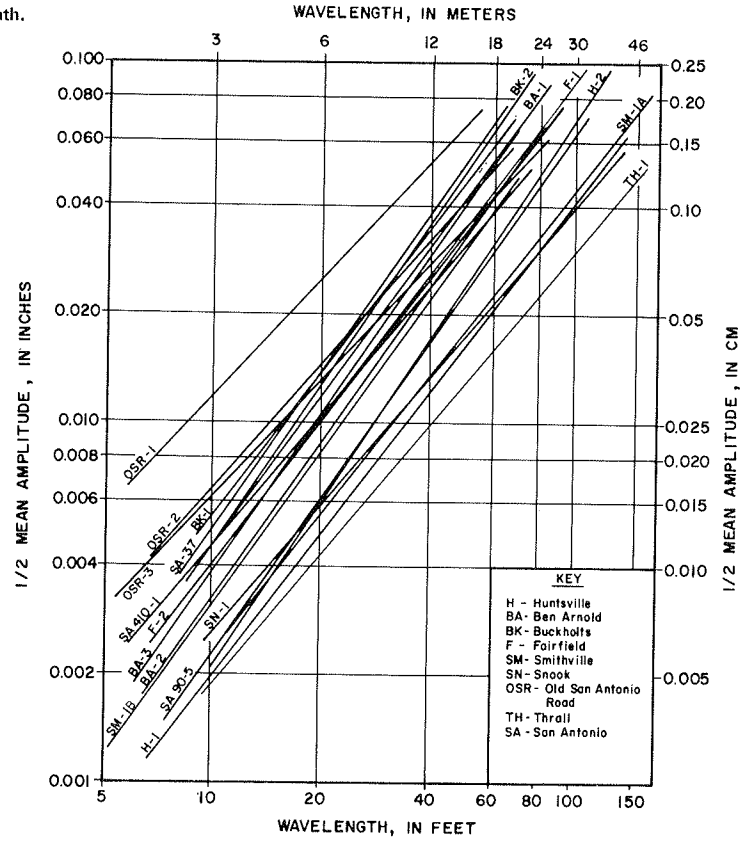

Figure 4. Comparison between roughness spectra for right and left wheel paths.

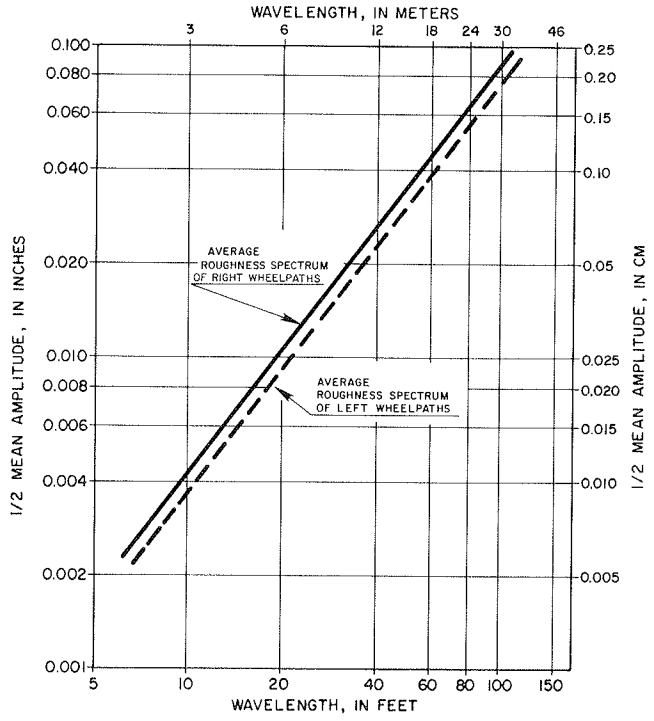

Figure 5. Log c versus n for right wheel path.

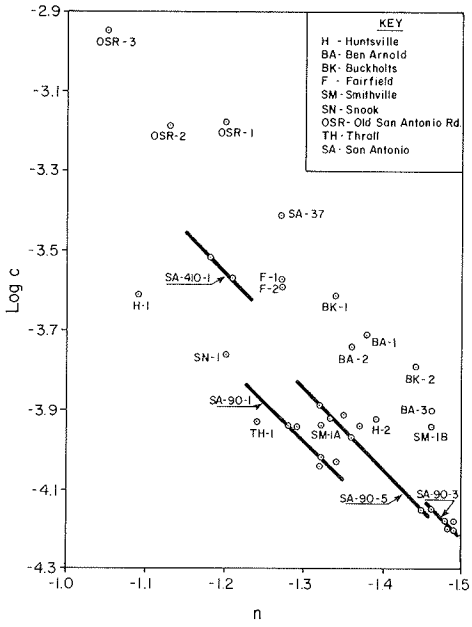

values of A/2 for the dominant wavelengths will appear as peaks above the fitted curves in the frequency-domain plots (Figure 1). Based on this assumption, the values of the dominant wavelengths have been estimated for the right wheel path of the different roadway segments and are given in Table 1. Even though the roadway sections have different characteristics, it appears that some of the dominant-wavelength values are the same for a significant number of sections. To illustrate this point, a bar graph was prepared that groups all the values included in Table 1 into 3-ft (1-m) intervals and calculates the percentage of dominant wavelengths in each interval with respect to the total number of values (see Figure 6). It appears that dominant

Table 1. Wavelengths of sinusoids with peak amplitude for right wheel path.

Section	Dominant Wavelengths[a] (ft)									
Huntsville										
1	9	11	13	16	22	30	42	52	-	-
2	8	11	14	17	-	28	38	52	70	-
Ben Arnold										
1	-	-	-	-	-	-	-	52	-	105
2	-	-	-	-	-	-	42	-	-	105
3	-	-	-	-	-	32	-	-	-	-
Buckholts										
1	-	-	12	-	-	-	-	-	84	-
2	-	-	-	-	-	-	42	-	-	105
Fairfield										
1	-	-	-	-	-	-	-	47	-	105
2	-	-	12	-	-	-	-	-	-	105
Smithville										
1A	-	-	-	-	-	-	42	-	-	105
1B	-	-	-	17	26	-	38	52	84	-
Snook 1	-	-	-	-	-	-	-	-	-	-
Old San Antonio Road										
1	8	9	-	-	-	30	38	-	-	-
2	-	10	-	20	-	32	-	-	60	-
3	-	10	12	-	26	35	-	52	-	-
Thrall 1	-	-	-	-	-	-	-	-	-	105
San Antonio										
410-1	-	-	12	20	-	-	-	-	-	105
37	-	-	-	-	-	30	-	47	-	105
90-5	-	-	-	-	-	-	38	52	-	-
90-3	-	-	-	-	-	-	-	-	-	105

Note: 1 ft = 0.3 m.

[a]From FFT analyses.

Figure 6. Distribution of dominant wavelengths from FFT analysis.

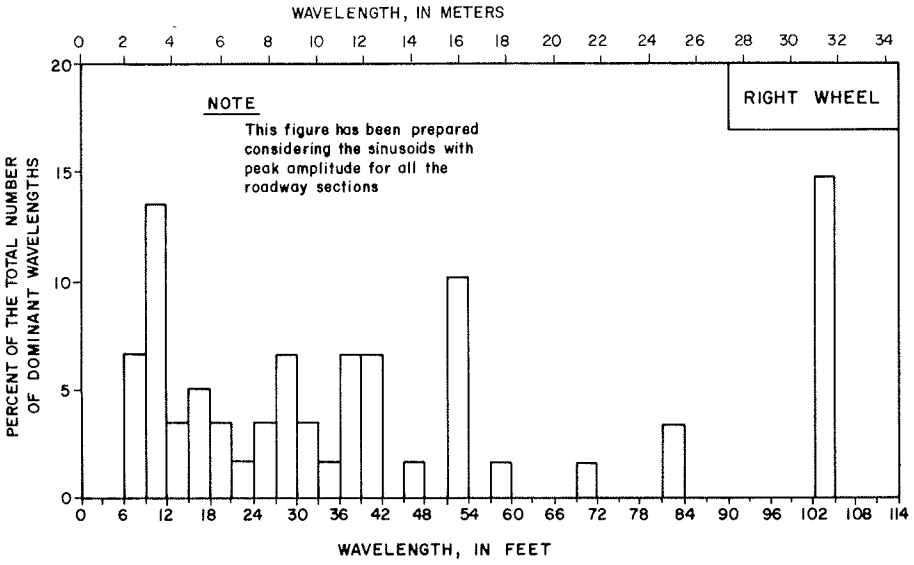

wavelengths are more frequent in the following intervals: 9-12 ft (3-4 m), 27-30 ft (8-9 m), 36-42 ft (11-13 m), 51-54 ft (16-17 m), and 102-105 ft (31-32 m).

It should be pointed out that the described technique (referred to here as technique A) for estimating dominant wavelengths has two drawbacks:

1. Since they are based on results of an FFT analysis, the estimated values represent sinusoidal components of the pavement roughness but not actual waves present in the road profile.
2. Given the characteristics of the input (sampling interval and number of samples) chosen in this study for the FFT analysis, the output is a distribution of sinusoids at discrete frequencies separated by 0.0024 cycles/ft (0.0079 cycles/m). With this frequency interval, actual short waves in the road profile will be distributed over several frequencies (and their possible amplitude peaks shadowed) while, on the other hand, the "resolution" in the lower frequency region is poor.

Because of these difficulties, it is convenient to use another approach (technique B) that complements the analysis of dominant wavelengths. This has been done by determining, directly on the road profiles, the wavelength probability density functions. A computer program with a special filter that copies the effect of a field survey (2) was used. The program scans through the profilometer data, finds the high points, and measures the horizontal distance between them. By using this information for each pavement section, the section's probability density functions of wavelength for both the right and left wheel paths can be calculated. One of these graphs is shown in Figure 7. It is assumed that dominant wavelengths will appear as relative maximums in the probability density functions. The values of the most noticeable maximums

in the probability density functions for the right wheel path are given in Table 2. Again, it seems that some of these values are the same for a significant number of roadway sections. To enhance this point, a bar graph was prepared that considers all of the values presented in Table 2 and calculates the percentage of dominant wavelengths in each 3-ft (1-m) interval with respect to the total number of values (see Figure 8). It appears that dominant wavelengths are most probable in the following intervals: 9-12 ft (3-4 m), 21-24 ft (6-7 m), 30-33 ft (9-10 m), and 45-48 ft (14-15 m).

A comparison between the results obtained from the two techniques used to distinguish dominant wavelengths is given below (1 ft = 0.3 m):

Technique	Dominant Wavelengths (ft)					
A	9-12	--	27-30	36-42	51-54	102-105
B	9-12	21-24	30-33	--	45-48	--

A general conclusion might be drawn from these results: Pavement roughness on expansive soils in central Texas seems to have dominant wavelengths of around 10 ft (3 m). Furthermore, these 10-ft waves also seem to combine, giving dominant waves with length multiples of 10 ft, especially around 30 and 50 ft (9 and 15 m).

Figure 7. Probability density function of wavelength (Buckholts 1 test section).

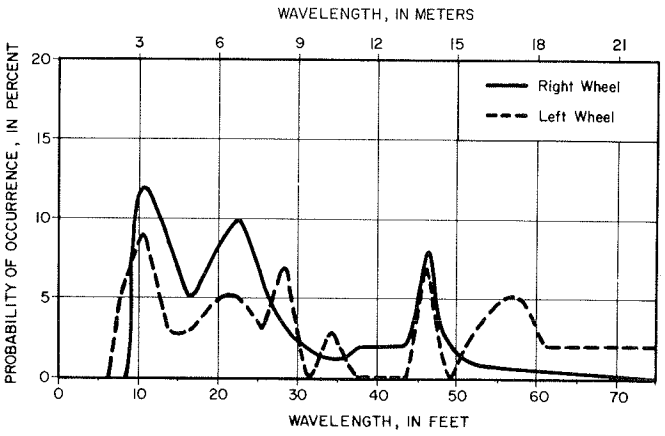

PREDICTION OF ROUGHNESS

It has been shown in this paper that pavement roughness can be described as a function of only two parameters, c and n. Several investigators have also noted this fact (5,7). Thus, the prediction of the parameters c and n is equivalent to the prediction of the pattern of roughness.

It is assumed that the flexural stiffness of the pavement, climate, time, and properties of the subgrade soils interrelate in the development of pavement roughness. Information about these factors

Table 2. Most probable wavelengths for right wheel path.

Section	Dominant Wavelengths[a] (ft)				
Huntsville					
1	10.5	16.5	22.5	-	-
2	10.5	-	22.5	31.5	-
Ben Arnold					
1	10.5	-	22.5	-	46.5
2	10.5	-	22.5	-	49.5
3	10.5	16.5	28.5	-	-
Buckholts					
1	10.5	-	22.5	-	46.5
2	10.5	-	-	31.5	37.5
Fairfield					
1	10.5	19.5	-	-	49.5
2	-	13.5	-	40.5	70.5
Smithville					
1A	10.5	19.5	-	37.5	-
1B	10.5	-	-	34.5	46.5
Snook 1	10.5	19.5	-	-	-
Old San Antonio Road					
1	10.5	-	22.5	31.5	46.5
2	10.5	19.5	-	31.5	-
3	10.5	-	22.5	-	-
Thrall 1	-	13.5	28.5	-	46.5
San Antonio					
410-1	9.0	16.5	25.5	34.5	-
37	10.5	-	-	31.5	58.5
90-5	10.5	19.5	-	-	52.5
90-3	10.5	-	28.5	-	55.5

Note: 1 ft = 0.3 m.

[a]Relative maximums in probability density functions.

Figure 8. Distribution of dominant wavelengths from probability density functions.

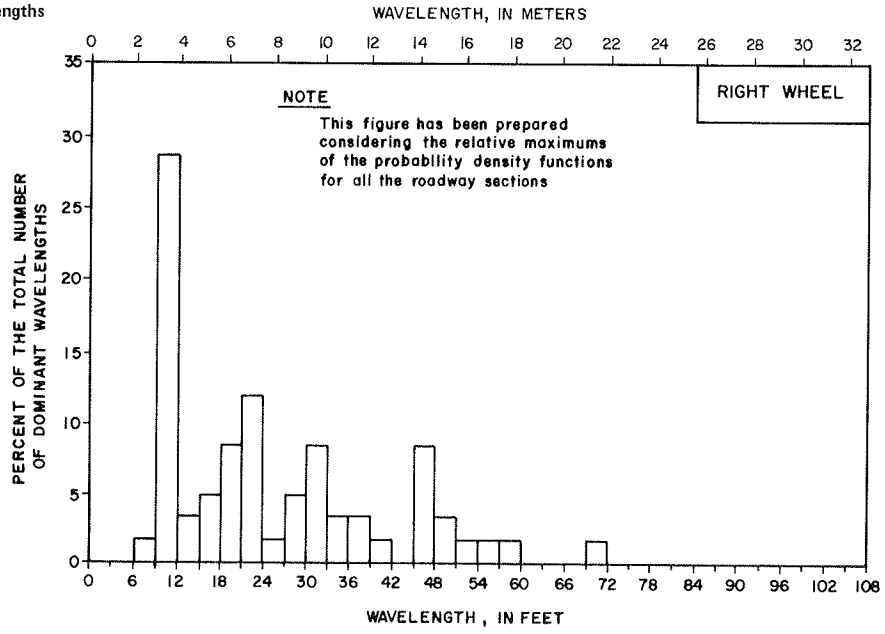

was collected for the different roadway sections.

The stiffness of a pavement depends on the type of materials and the depths of the surface and base courses. The fact that pavements are multilayered systems that have different materials complicates their direct comparison. To overcome this problem, a simple approach was used: determining for each pavement its "effective depth", a homogeneous quantity related to stiffness (the greater the depth, the stiffer the pavement). To define this quantity, the following process was used:

1. The values of the modulus of elasticity were assumed for the different materials involved. Asphalt concrete was the material chosen as a basis for subsequent comparisons. The assumed moduli of elasticity are (a) for asphalt concrete (E_0), 200 000 lbf/in² (1400 MPa); (b) for base (E_b), 30 000 lbf/in² (210 MPa); and (c) for surface materials (E_s), as given below (1 lbf/in² = 0.007 MPa):

Material	E_s (lbf/in²)
Asphalt concrete	200 000
Concrete	3 000 000
Double bituminous treatment	100 000

2. Given a pavement structure 1 in (2.5 cm) wide (see Figure 9), an equivalent configuration is defined based on the moduli-of-elasticity ratios E_s/E_0 and E_b/E_0. The dimensions of this hypothetical configuration are shown in Figure 10.

3. The moment of inertia (I) for the equivalent configuration is calculated. Finally, the "effective depth" (in inches) is defined as

$$\text{DEPTH} = \sqrt[3]{(12 \times I)/1 \text{ in}} \quad (4)$$

The calculated effective depths for the different pavement sections are presented in Table 3.

The mean Thornthwaite Moisture Index (TH) values for a 20-year period in the different counties where the pavement sections are located have been recorded and considered as environmental indicators. Moreover, the ranges of the TH values for the same 20-year period have been recorded and considered as rough indicators of climate variability in the different areas.

In addition, the dates of construction and subsequent repair (if any) of the pavements are known. This information is needed in the analysis of roughness as a time-dependent problem.

The subgrade soils in 13 sections belong to the Vertisol order. Alfisols underlie the remaining 7 roadway segments. All of these soils have been evaluated by soil scientists as having a high or very high shrink-swell potential. Soil samples were taken adjacent to the roadway segments at depths of

Figure 9. Pavement structure.

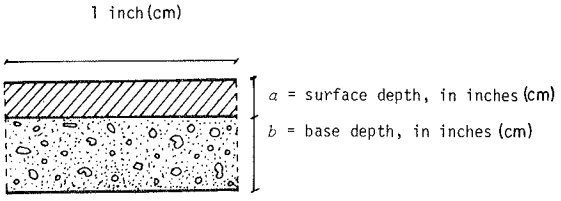

Figure 10. Equivalent pavement configuration based on moduli-of-elasticity ratios.

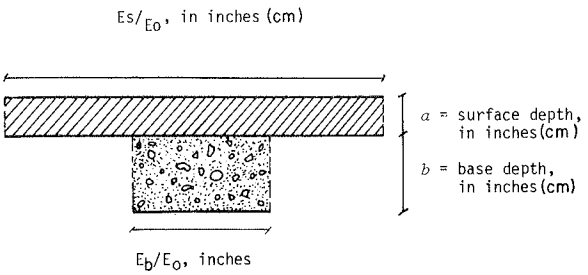

Table 3. Calculated effective depth of pavement test sections.

Section	Type of Pavement	Depth (in)		Moduli-of-Elasticity Ratio		Effective Depth (in)
		Base	Surface	E_b/E_0	E_s/E_0	
Huntsville						
1	Concrete	8	8	0.15	15	20.5
2	Concrete	8	8	0.15	15	20.5
Ben Arnold						
1	Asphalt concrete	14	2.3	0.15	1	10.9
2	Asphalt concrete	14	2.3	0.15	1	10.9
3	Asphalt concrete	14	2.3	0.15	1	10.9
Buckholts						
1	Asphalt concrete	16	1.6	0.15	1	11.5
2	Asphalt concrete	16	1.6	0.15	1	11.5
Fairfield						
1	Concrete	6	8	0.15	15	20.2
2	Concrete	6	8	0.15	15	20.2
Smithville						
1A	Asphalt concrete	24	1.2	0.15	1	15.6
1B	Asphalt concrete	24	1.2	0.15	1	15.6
Snook 1	Asphalt concrete	7	1.1	0.15	1	5.4
Old San Antonio Road						
1	Double bituminous treatment	6	0.6	0.15	0.5	4.0
2	Double bituminous treatment	6	0.6	0.15	0.5	4.0
3	Double bituminous treatment	6	0.6	0.15	0.5	4.0
Thrall 1	Asphalt concrete	13	3.1	0.15	1	11.1
San Antonio						
410-1	Asphalt concrete	21	-[a]	0.15	1	-
37	Concrete	8	8	0.15	15	20.5
90-5	Asphalt concrete	32	3	0.15	1	20.9
90-3	Asphalt concrete	23	3.5	0.15	1	17.7

Note: 1 in = 2.5 cm.

[a]Unknown.

Table 4. Results of soils tests for roadway segments.

Section	Percentage Clay[a]	Liquid Limit	PI	CEC (meq/100 g)	ESP (%)
Huntsville					
1	27	33	15	25	6.0
2	50	71	49	46	2.0
Ben Arnold					
1	65	82	51	74	10.0
2	69	88	54	61	3.0
3	66	75	45	64	0.9
Buckholts					
1	60	79	50	48	16.1
2	53	57	35	44	6.0
Fairfield					
1	40	45	26	39	5.0
2	47	46	27	38	4.0
Smithville					
1A	57	68	44	52	2.3
1B	69	84	56	54	9.7
Snook 1	57	71	44	58	0.5
Old San Antonio Road					
1	58	58	38	50	0.6
2	50	57	35	46	0.5
3	66	80	50	74	0.7
Thrall 1	50	53	28	74	0.6
San Antonio					
410-1	53	72	42	43	15.3
37	49	62	38	56	4.2
90-5	48	86	50	68	16.3

[a]Percentage smaller than 0.002 mm.

1, 2, and 3 ft (0.3, 0.6, and 0.9 m). The following tests were performed: (a) Atterberg limits, (b) determination of percentage clay (grain size less than 0.002 mm), (c) cation exchange capacity (CEC), and (d) exchange sodium percentage (ESP). The average test results for each roadway segment are given in Table 4, except for San Antonio 90-3, where samples of the natural soils were not taken. Knowing the plasticity index (PI), CEC, and percentage clay of a soil, its activity (PI ÷ percentage clay) and cation exchange activity (CEC ÷ percentage clay) can be calculated. The chart developed by McKeen (6) allows the estimation of the coefficient of linear extensibility (COLE) of a soil as a function of these two quantities. The chart is shown in Figure 11.

Prediction Models

Empirical models to predict c and n (for both the right and left wheel paths) have been derived by considering 10 possible independent variables:

DEPTH = effective depth of pavement (in),
TH = mean value of Thornthwaite Moisture Index for a 20-year period,
RANGE = range of values of Thornthwaite Moisture Index for a 20-year period,
TIME = time since construction or last rehabilitation before the roughness was measured (years),
CLAY = percentage clay (grain size less than 0.002 mm),
AC = activity (PI/CLAY),
CEC = cation exchange capacity (meq/100 g),
CEAC = cation exchange activity (CEC/CLAY),
COLE = coefficient of linear extensibility, and
ESP = exchange sodium percentage.

To determine the prediction models, the SELECT regression program (8) has been used. Given sets of values for the dependent variable y and the independent variables x_1, x_2, ..., x_n, the program uses a linear regression technique to find

Figure 11. Chart for COLE prediction.

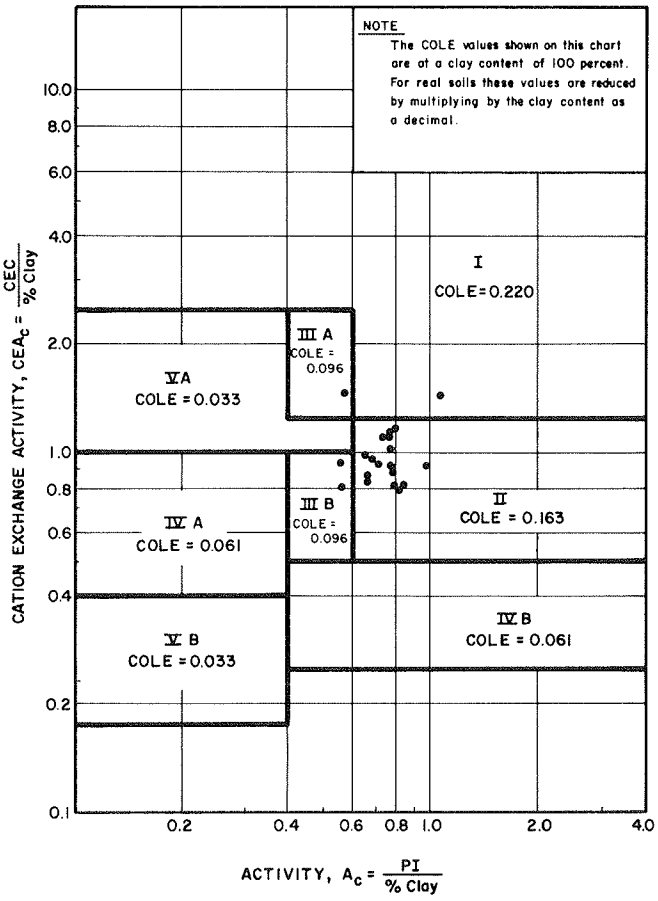

models using n, n - 1, n - 2, and so on down to 1 indepen- dent variables. In this case, 17 sets of values were input to the SELECT regression because three sections were eliminated from the regressions: San Antonio 410-1, where it was not possible to estimate the effective depth; San Antonio 90-3, which is on fill; and San Antonio 90-5, where the subgrade was ponded prior to construction.

Simplicity, high multiple correlation, and physical meaning have been the criteria followed to choose the best models to predict the parameters c and n. These empirical prediction models are as follows: For the left wheel path,

$$c = 0.0008\ DEPTH^{-1.07} TIME^{0.30} AC^{-1.04} ESP^{0.19} \quad (R^2 = 0.78) \quad (5)$$

$$n = -1.06\ DEPTH^{0.13} CEC^{-0.17} CLAY^{0.32} (TH + 35)^{0.16} RANGE^{-0.30} \quad (R^2 = 0.86) \quad (6)$$

For the right wheel path,

$$c = 0.0004\ DEPTH^{-0.81} TIME^{0.49} AC^{-1.20} ESP^{0.12} \quad (R^2 = 0.77) \quad (7)$$

$$n = -0.79\ DEPTH^{0.09} CEC^{-0.16} CLAY^{0.40} RANGE^{-0.16} \quad (R^2 = 0.83) \quad (8)$$

To interpret these equations properly, it should be noted that an increase in the c value represents a proportional increase in amplitude for all the wavelengths in the roughness spectrum. An increase in the absolute value of n represents a proportionally higher amplitude increase of the long wavelengths than of the short wavelengths. Besides, n and c are not truly independent. With these facts

Figure 12. Sensitivity of SI-reduction model to CLAY and DEPTH variables (San Antonio 90-5 test section).

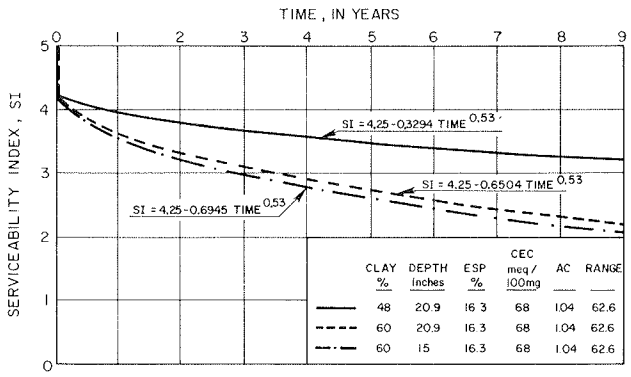

in mind, several observations about the prediction models can be made:

1. DEPTH influences the development of roughness. An increase in DEPTH causes an appreciable decrease in the c values and a minor increase in the absolute values of n. As a result, the stiffer the pavement, the less roughness will develop, especially with the shorter wavelengths.
2. Roughness increases with time.
3. As RANGE increases, the absolute value of n decreases. This fact seems to indicate that climate variability enhances the relative importance of the short wavelengths with respect to the long wavelengths.
4. TH is included only in the model for the parameter n in the left wheel path. This probably indicates that the long-term average climate, which corresponds to equilibrium conditions, has a greater influence on the roughness developed in the center of the pavement than that at the borders.
5. The influence of the soil properties in the models is reflected through the variables ESP, AC, CEC, and CLAY. As ESP increases, roughness increases. The other three soil variables are not truly independent. Their effects should be considered as a group. Nevertheless, it appears that a higher clay content causes high roughness, especially in the long waves. On the other hand, CEC and AC (with minor influence) appear to have the opposite effect. Thus, the models show the complication of the physicochemical phenomena that take place in the development of roughness, which cannot be explained only as a function of a single soil property.
6. The values of the parameter n are probably related to the soil crack spacing.

Correlation with Serviceability Index

Various highway departments decide to rehabilitate a road when the serviceability index (SI) drops below 2.5-3.0. Then the prediction of the SI decrease with time is a critical aspect in the definition of the optimum strategy to follow in order to minimize the overall cost of the expected life of the road. Lu and others (9) have developed a methodology and presented models to predict serviceability loss of flexible pavements as a result of fatigue, swelling and shrinkage, and thermal cracking.

A simpler approach to estimation of the reduction in the SI (ΔSI) is presented here, based on the correlation between ΔSI and the parameters c and n for the right wheel path, which in turn can be predicted by using the models given as Equations 5-8.

In eight roadway sections, the values of the SI are known. Multiple regression analysis has been performed to obtain the following equation:

$$\Delta SI = 2675.41\, c^{1.09}|n|^{7.62} \quad (R^2 = 0.73) \tag{9}$$

As expected, ΔSI increases as c or |n| increases. Moreover, the right-wheel-path prediction models for c and n can be substituted in Equation 9. The obtained equation is then

$$\Delta SI = 0.087\, DEPTH^{-0.20} TIME^{0.53} ESP^{0.13} CEC^{-1.22} \times CLAY^{3.05} AC^{-1.31} RANGE^{-1.22} \tag{10}$$

Although riding quality depends on other factors besides the roughness of the right wheel path, Equation 10 permits approximate prediction of the decrease in SI as a function of the characteristics of the pavement, time, subgrade soil properties, and climate. Thus, the equation can be used as the basis of a design procedure. If one knows the climate and subgrade soil properties, it is possible to estimate (by trial and error) the combination of base and surface thicknesses needed to maintain the SI above a specific value for a specific length of time after construction.

Finally, to show the sensitivity of the SI-reduction model to the values of the DEPTH and CLAY variables, three curves are shown in Figure 12. One of the curves has been calculated by using the actual values of the variables for the San Antonio 90-5 section and by assuming that the SI was equal to 4.25 at the end of construction. The second curve has been determined by varying only the value of CLAY (CLAY = 60 instead of 48 percent) and the third curve by changing the values of CLAY and DEPTH [CLAY = 60 percent and DEPTH = 15 in (38.1 cm) instead of 20.9 in (53.1 cm)]. It can be observed in Figure 12 that the variable CLAY has an appreciable effect on the reduction of the SI whereas the variable DEPTH has a less important influence.

CONCLUSIONS

1. The FFT method, used to study the road profiles in the frequency domain, is a powerful analytic tool.
2. Pavement roughness along each wheel path can be characterized as a function of only two parameters, c and n.
3. The parameters c and n are not independent.
4. Dominant waves in the pavements studied are approximately 10 ft (3 m) long. Furthermore, these 10-ft waves seem to combine, giving also dominant waves with length multiples of 10 ft, especially around 30 and 50 ft (9 and 15 m).
5. Empirical models for predicting c and n have been developed. These models indicate how the stiffness of the pavement, time, climate, and several physicochemical soil properties interrelate in the development of pavement roughness. Percentage clay, time, effective depth of the pavement, and ESP appear to be the more influential variables in the development of roughness.
6. The values of the parameters c and n for the right wheel path have been correlated with reduction in SI. This correlation and the prediction models for c and n also make it possible to estimate the reduction in SI.
7. The methodology presented in this study has practical applications in the design of pavements on expansive soils. A computer program can be designed to calculate the combination of base and surface thicknesses needed to maintain the SI above a specific value for a specific length of time after construction.

8. The prediction models have been obtained from data collected on pavement sections in cut and at grade with no protective measures to reduce swelling. On the other hand, research is now under way on some test sections where ponding was conducted prior to construction or vertical moisture barriers have been implemented. The models can help in the evaluation of these measures by comparing the actual roughness developed with that predicted. In the future, when more data are available, the models can be improved to account for the effects of protective measures, pretreatments, presence of fill, or rebound of deep excavations.

REFERENCES

1. G.G. Beckmann, G. Hubble, and C.H. Thompson. Gilgai Forms, Distribution, and Soil Relationships in North-Eastern Australia. Proc., Symposium on Soils and Earth Structures in Arid Climates, Institution of Engineers, Adelaide, Australia, May 1970, pp. 88-93.
2. R.L. Lytton, R.L. Bogges, and J.W. Spotts. Characteristics of Expansive Clay Roughness of Pavements. TRB, Transportation Research Record 568, 1976, pp. 9-23.
3. D.M. Patrick and D.R. Snethen. An Occurrence and Distribution Survey of Expansive Materials in the United States by Physiographic Areas. Federal Highway Administration, U.S. Department of Transportation, Rept. FHWA-RD-76-82, Jan. 1976.
4. E.O. Brigham. The Fast Fourier Transform, 1st ed. Prentice-Hall, Inc., Englewood Cliffs, NJ, 1974.
5. B.E. Quinn and S.A. Sattaripour. Measurement and Prediction of the Dynamic Tire Forces of a Passenger Vehicle on a Highway. Federal Highway Administration, U.S. Department of Transportation, Rept. FHWA-RD-72-26, Aug. 1972.
6. R.G. McKeen. Field Studies of Airport Pavements on Expansive Clay. Proc., 4th International Conference on Expansive Soils, Denver, CO, ASCE, New York, Vol. 1, June 1980, pp. 242-261.
7. A.D. Brickman, J.C. Wambold, and J.R. Zimmerman. An Amplitude-Frequency Description of Road Roughness. In Improving Pavement and Bridge Deck Performance, HRB, Special Rept. 116, 1971, pp. 53-67.
8. D.A. Debuse. Variable Selection Procedure: Implementing the Hocking-LaMotte-Leslie Method. Institute of Statistics, Texas A&M Univ., College Station, 1970.
9. D.Y. Lu, R.L. Lytton, and W.M. Moore. Forecasting Serviceability Loss of Flexible Pavements. Texas Transportation Institute, Texas A&M Univ., College Station, Res. Rept. 57-1F, Nov. 1974.

Publication of this paper sponsored by Committee on Environmental Factors Except Frost.

Deep-Vertical-Fabric Moisture Barriers in Swelling Soils

MALCOLM L. STEINBERG

A deep-vertical-fabric moisture barrier has been placed on two Texas highways that have been severely damaged by swelling-soil subgrade. Previous testing of a ponding section has indicated the depth of the zone of activity. By developing additional mechanisms and making maximum use of prior developments, the Texas State Department of Highways and Public Transportation is using fabric on two San Antonio freeway rehabilitation projects: an 0.8-km (0.5-mile) test section on Interstate Highway Loop 410 and a 3.2-km (2-mile) section of I-37. DuPont EVA-coated Typar T063 fabric has been placed 2.4 m (8 ft) into the zone of activity. The goal is to minimize destructive pavement movements over expansive clays by minimizing moisture change. Testing includes moisture-sensor readings, profilometer measurements computer converted to serviceability indexes, photologging, elevation readings, and pavement surface inventories. There are no reportable results for the recently completed I-37 project. However, after a two-year testing span on Loop 410, profilometer serviceability indexes and other favorable measurements indicate a better riding surface on the fabric-protected lanes than on the adjacent control section. The results are viewed with guarded optimism.

Expansive soils are estimated to cause between $7 and $9 billion/year in damages in the United States (1, p. 596). More than half of these damages are to transportation facilities, highways, railroads, airports, pipelines, canals, and sidewalks (2).

The problems of swelling soils are worldwide. Expansive soils occur in Australia, South Africa, South America, India, Israel, Poland, Canada, and in the United States, where they occur from border to border and coast to coast.

These soils have spawned many tests, reports, papers, international conferences, meetings, and cures. One of the more complete literature reviews was part of a study done by the U.S. Army Engineer Waterways Experiment Station (WES) for the Federal Highway Administration (FHWA) (3).

Texas has its share of swelling soils. Like many other agencies, universities, and consultants, the Texas State Department of Highways and Public Transportation (TSDHPT) has tried many cures and methods and has reported on them (4). The department has continued to work cooperatively with Texas A&M University, the Texas Transportation Institute (TTI), the University of Texas, the Center for Transportation Research, FHWA, and the WES project to seek solutions to this problem.

Another significant contribution of the WES study was the development of national and regional maps that show the relative occurrence of swelling soils (5). These are invaluable data. They must be viewed, however, with an awareness that they provide generalized information rather than a rigid rule. For example, if one examines the WES map of Texas, the El Paso area in the far western corner is noted as being lightly impacted by swelling soils (see Figure 1). Yet, in one residential development in this area, more than 100 homes were severely damaged as a result of expansive soils. These builders and buyers did not feel "lightly impacted"!

Tests with the deep-vertical-fabric moisture barrier (DVFMB) are being conducted by TSDHPT, in cooperation with Texas A&M University and TTI, in the San Antonio area of south-central Texas (see Figure 2). The city is in Bexar County, 200 km (125 miles) from the Gulf of Mexico. Since meteorologic and geologic conditions are so closely related to the